Finite Element Analysis of Bicycle Crank Arm on the Mechanical Aspect

M.U. Rosli[1]* and S. Zulkifli[1]

[1]Faculty of Mechanical Engineering and Technology, Universiti Malaysia Perlis, 02600 Perlis, Malaysia

ABSTRACT

The demand for increased performance both in the professional and amateur sectors and the inclusion of the bicycle in the city as a clean, silent, inexpensive, and healthy personal transport, is responsible for the technological growth of the industry. This study aims to analyze the effect of the design parameters on the bicycle crank arm and to find the best design value within the range for minimal defects. The strength of the structure design is significant to ensure the performance of the bicycle crank arms. To solve this problem, several design structures and parameters were studied. The selected parameters in this study are crank arm length, width, thickness, number of cranks spider, and rib design. Von-misses stress, strain, and displacement are selected as dependent variables. Aluminium Alloy 6061-T6 is the selected material in this study. The external load of 1000 N force was applied in the y-direction. The length analysis results show that 160 mm length, 30 mm width, and 10 mm thickness with five crank spiders and pocket design arm have the lowest stress, strain, and displacement. By bringing a new alternative to the crank's arm structure, the cost of the manufacture will be reduced. At the same time, it can help precisely improve the rigidity of producing complex 3D shapes.

Keywords: Finite element analysis, Bicycle crank arm, Simulation, Mechanical aspect

1. INTRODUCTION

In recent years, the cycling industry has made a breakthrough. For the technological growth of the industry, the requirement for increasingly demanding performance in both the professional and amateur sectors and the inclusion of the bicycle in the city as a smooth, silent, cheap, and healthy private transport is responsible [1]. In professional cycling, minimal weight and structural rigidity are required to improve elite athletes' performance. Hence, several productions of the structural elements of the bicycle use different materials such as aluminum, titanium, and carbon fibers. In modern engineering, it is necessary to identify all possible sources of uncertainty since there is better control of the experimental test and the theoretical model to be validated. The possible sources of uncertainty in validating the results had not been considered in the different studies on bicycle components. This was the wake-up call for safe and robust products in these studies.

Today, cycling is not just restricted to road riding. However, it can be seen in road bikes, mountain bikes, sports, or many unfavorable situations. Because the arm of the crank is the component on which riders' balance lies in motion, imagine a situation when someone gets lost while stunting or driving on a steep, narrow mountain due to crankshaft failure; it may lead to severe wounds or death. Fortunately, using finite element analysis (FEA) renders quick economic and authentic means of predicting and solving fatigue issues in these studies. Crank arm failure was the bicycle's most critical failure point [2]. The performance of crank arms depends on the bicycle's weight and design [3]. Crank arms can therefore be cracked in several places. Crank arm failure means

that its mechanical strength suddenly deteriorates due to loading effects. The material strength should nevertheless be able to cope without fail with applied stress. The von Misses stress, strain, and displacement can be applied to the load. Crankarms play a significant part in transferring force to the crankset from the pedals.

In past research, Gutiérrez-Moizant et al. (2020) studied comparing the finite element model with the experimental results of a bicycle crank arm. In a universal dynamic test bench, the structural integrity of the crank arm was analyzed to know the component tiredness behavior [4]. Ismail et al. (2020) applied topology optimization and surface response methods to optimize the geometry of and experimental validation of the bicycle crank arm [5]. This is intended to reduce the crank arm's weight and develop a preliminary lightweight structure for high-performance cycling. McEwen et al. (2018) enhanced the approach of optimizing the topology on a bicycle crank arm with an additional optimization method to improve the design [6]. After the optimized topology is obtained, the additional response surface method is used to reduce stress concentrations. The optimized design was finally validated experimentally. Htun and Nyi. (2019) analyzed crank arm structural analysis using three different materials [7]. The problems in designing and simulating the crank arm optimization with stiffness and strength constraints are considered for design security using SolidWorks software. According to Charan and Garg (2019), geometry was refined by using the method of body sizing till receiving the converged result of maximum stress. This study proposed design improvements concerning minimizing the crank arm's defect [8].

In a current study, the effect of the design parameters on mechanical performance was analyzed using finite element simulation [9]. Simulation analysis intends to verify that the product meets its requirements for operation. It can further provide insight into necessary changes and validate that the correct real-world tests are conducted, especially in engineering fields such as mechanical and electronic products [10, 11]. The selected parameters in this study are crank arm length, width, thickness, number of cranks spider, and rib design. This study selected Von Misses stress, strain, and displacement as dependent variables.

2. METHODOLOGY

3D modeling procedures of the crank arm using SolidWorks are shown in Figure 1. This undergoes a sketching and redesign process. After the 3D model is meshed and validated, the analysis is carried out based on the selected crucial design parameters: crank arm length, width, thickness, number of cranks spider, and rib design. SolidWorks simulation was used to study the effects of von Mises stress, displacement, and strain. After comparing the results between each level of design, the data will be analyzed using regression analysis, a statistical technique for assessing correlations between design parameters and mechanical weaknesses.
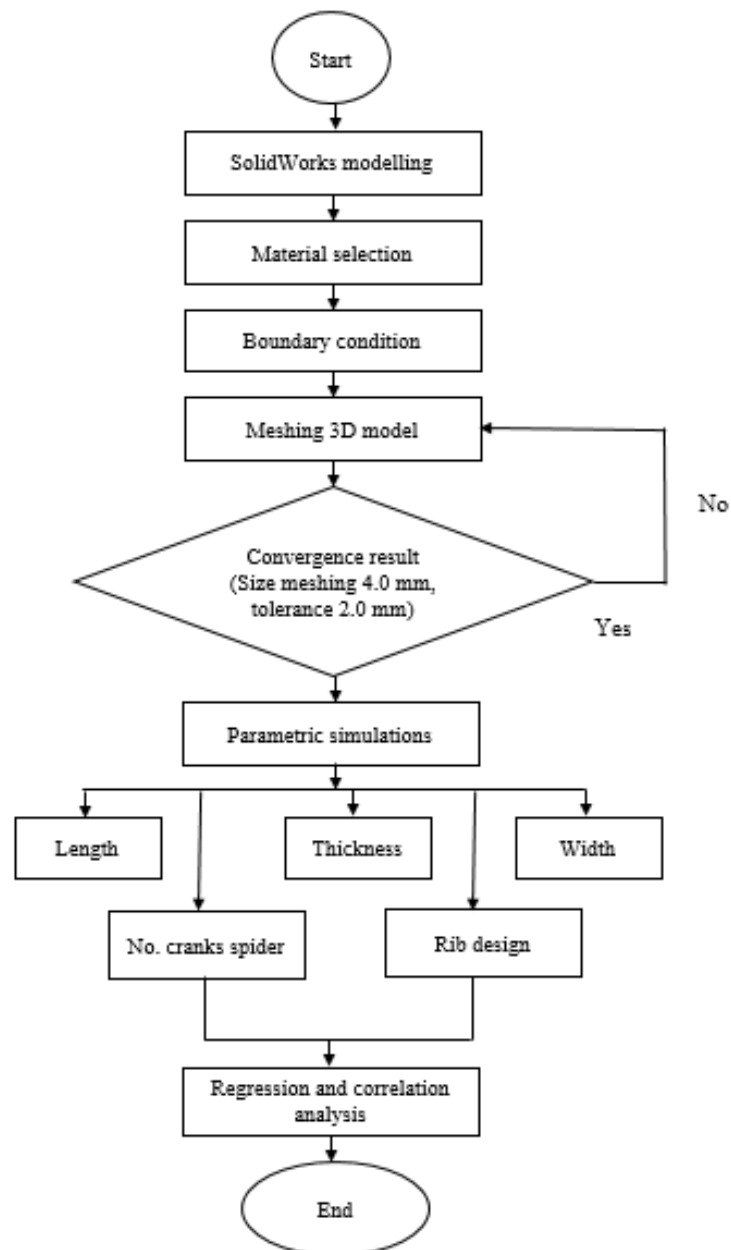
Figure 1: Flow chart of the finite element analysis.

2.1 Solidworks Modeling

The bicycle crank arms analysis will be designed and simulated in this study using SolidWorks. This software covers all detail drawing to the extent of mm level sketch line and accuracy. This software can create simulations that test a product's durability, strength, and static properties [7]. SolidWorks simulations were used to determine the deflection and other static analysis of crank arms when external force acts on them. Simulation studies were carried out in the y-direction. The length of the crank arms structure is 170 mm, and the force distribution of 1000 N was applied to investigate the von Misses stress, strain, and displacement structure. For a professional cycling crank, the load varies from 0 N to 1800 N with a maximum frequency of 25Hz [1]. SolidWorks modeling is shown in Figure 2 and Figure 3.
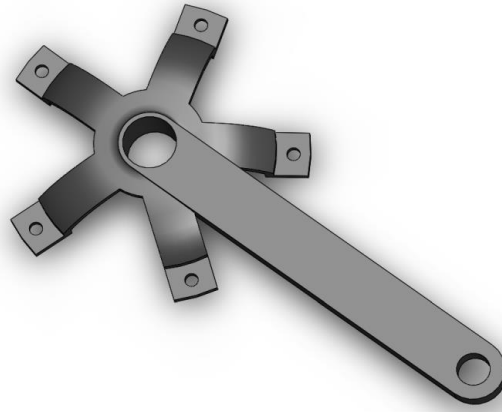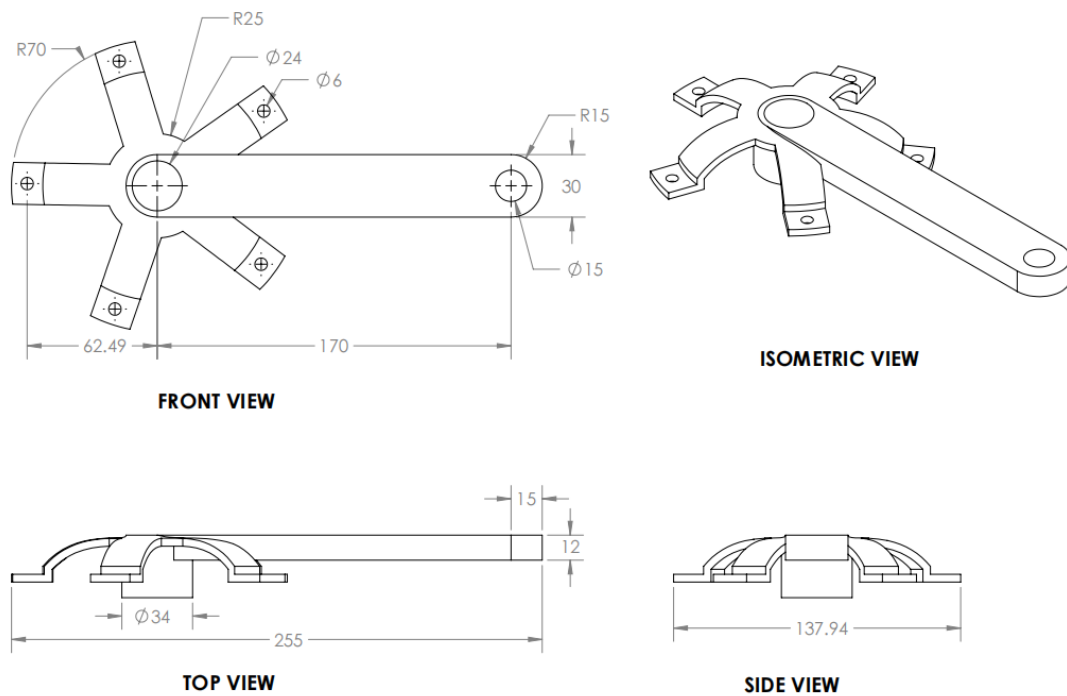
Figure 2: Crank arm in 3D view.

Figure 3: Crank arm drawing (mm).

2.2 Boundary Condition

The component listed below is the sub-component that is involved in the boundary condition. It is the part to define the simulation boundary conditions and all the related simulation parameters. The generated mesh was imported, and all the conditions were defined. The materials should be defined correctly with all the physical properties required by the model. The materials of this crank arms structure are AA6061-T6. The structure on the crank arm's length is 170 mm and was loaded by a distributed force of 1000 N on the crank's hole between the support, as shown in Figure 4. This is loading in a vertical plane at the x–z plane to construct the weight of components distributed along the crank, which causes bending about the y-axis [6]. To investigate the behaviors in structure or component caused by loads, the static structural analysis was used to determine the von-misses stress, strain, and displacement. The variable force acting on the crank's hole is 1000N [6].
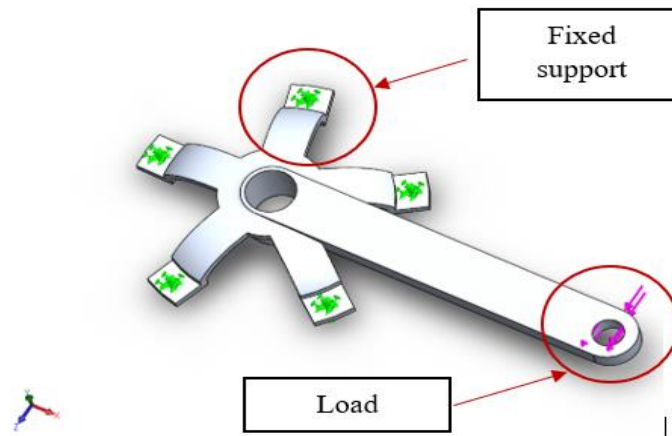
Figure 4: Fixed supports on the crank arm.

2.3 Meshing 3D model

For simulation, SolidWorks meshing technology can provide a means to balance the requirement. The meshing process will divide the geometry into an element, and afterward, the SolidWorks simulations use the elements that are generated to calculate the value of each node. The finite element model of the structure is established using the multi-Zone process. This geometry model has meshed and was imported for the structural analysis. Figure 5 shows the generated mesh around the geometry. The size element for the meshing is 4.0 mm, and the tolerance is 0.20 mm.
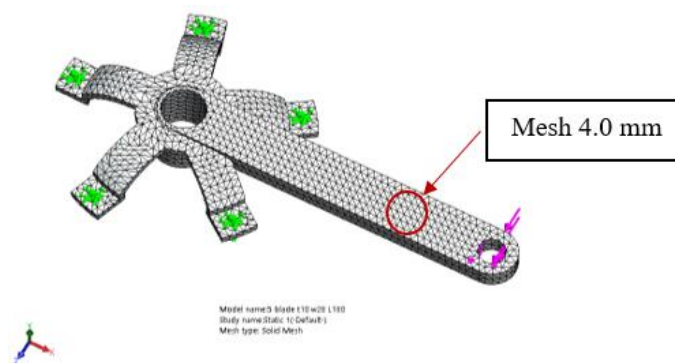

Figure 5: Meshing on the crank arm.

Grid sensitivity test can be considered to obtain a more optimal grid element which can bring a more consistent result. There is a number of grid tests that need to be done before further analysis. Thus, it is necessary to perform the mesh independency test to get the optimum size of the grid for a more accurate result. Mesh with lower grid elements will significantly minimize the computational analysis's time consumption. For the grid independence test, parameters such as length, width, thickness, number of cranks spider, rib design, and material are fixed at constant.

2.4 Range selection of each factor

The crank arm model was designed and labeled based on Table 1 and Figure 6. Five parameters were considered in the simulation analysis. Each parameter was defined with three levels, as summarized in Table 1. Length, thickness, width, number of cranks spider, and rib designs of the crank arm were selected.
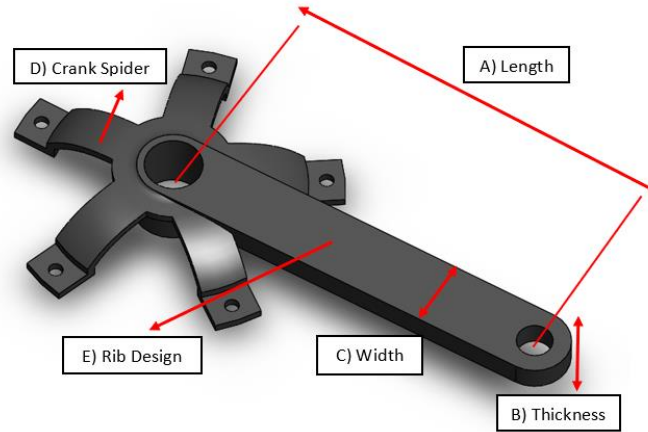
Figure 6: Selection of factors on the crank arm.

Table 1: Range of measurement in the bicycle cranks arm.

Parameters	Level 1	Level 2	Level 3
Lengths	160 mm	170 mm	180 mm
Thickness	10 mm	12 mm	14 mm
Widths	28 mm	30 mm	32 mm
No. crank spider			
Rib design			

3. RESULTS AND DISCUSSION

3.1 Analysis of factor A: Arm length

In this analysis, only the arm length varies (160 mm, 170 mm, 180 mm), and the other factor is fixed on the level 2 value. All simulations were performed with an external load of 1000 N force. The result of von Mises stress, displacement, and strain are shown in Figures 7 (a), (b), and (c), respectively. Based on the graph shown in Figure 7(a), the highest stress is 437.1 MPa for 180 mm length, and the lowest is 350 MPa for 160 mm length. The percentage of difference for both levels in the y-direction was approximately 11.06%. Figure 7(b) shows that when 1000 N force was applied, the strain on 180mm length was the highest (4.048×10^{-3} mm) compared to 160 mm length (3.206×10^{-3} mm). The percentage of difference for both structure levels in the y-direction was approximately 11.6%. For displacement, as shown in Figure 7(c), the highest displacement is 2.427 mm for 180 mm length, and the lowest is 1.731 mm for 160 mm length. The percentage difference for both structure levels in the y-direction is approximately 6.85%. From these length analysis results, it can be concluded that decreasing the length will also decrease the stress, strain, and displacement value. Moreover, shorter cranks will help most riders be more comfortable on a bike. Past research also found that riders reached their peak power nearly 1 second quicker on 170 mm cranks than on 180 mm cranks [12]. Shorter cranks give riders better acceleration, which can make a difference when passing other riders or trying to clean an obstacle.
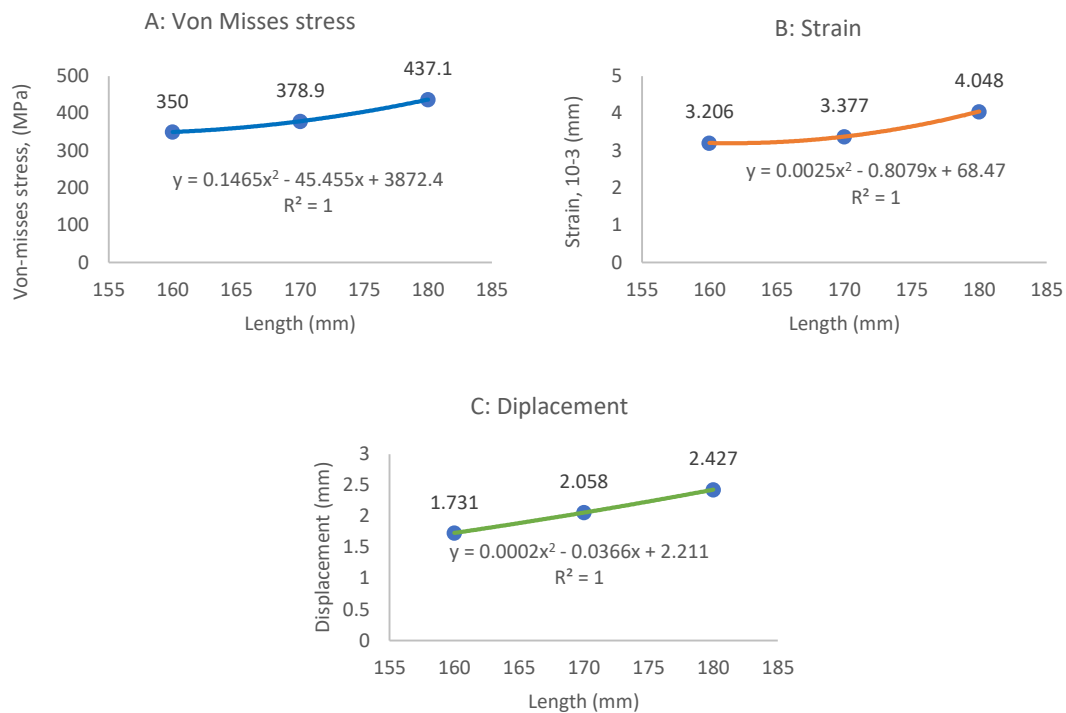
A: Von Misses stress

B: Strain

C: Diplacement

Figure 7: (a) maximum von Mises stress, (b) displacement, and (c) strain for length analysis.

3.2 Analysis of factor B: Thickness

Another static analysis that was investigated through simulation studies is thickness. In this analysis, only the thickness varies (10 mm, 12 mm, 14 mm), and the other factor is fixed on the level 2 value. All simulations are performed with an external load of 1000 N force. The result of von Mises stress, displacement, and strain are shown in Figures 8 (a), (b), and (c), respectively. Based on the graph shown in Figure 8 (a), the highest stress is 14 mm arm thickness with 430.7 MP; the lowest is 10 mm arm thickness with 379.1 MPa. The percentage of difference for both levels is approximately 6.38%. This result shows that 14 mm thickness has a more significant area to endure the external force. Based on the graph illustrated in Figure 8 (b), the strain on width 14 mm is the highest (3.950×10^{-3} mm) compared to 10 mm (3.639×10^{-3} mm). The percentage difference for both structure levels is approximately 4.22%. Based on the graph in Figure 8 (c), the displacement on thickness 14 mm is the lowest (1.882 mm) compared to 10mm (2.312 mm). The percentage of difference for both structure levels in the y-direction is approximately 10.26%. These thickness analysis results show that increasing the arm thickness will increase the stress and strain value. However, the displacement value decreased when the thickness increased.
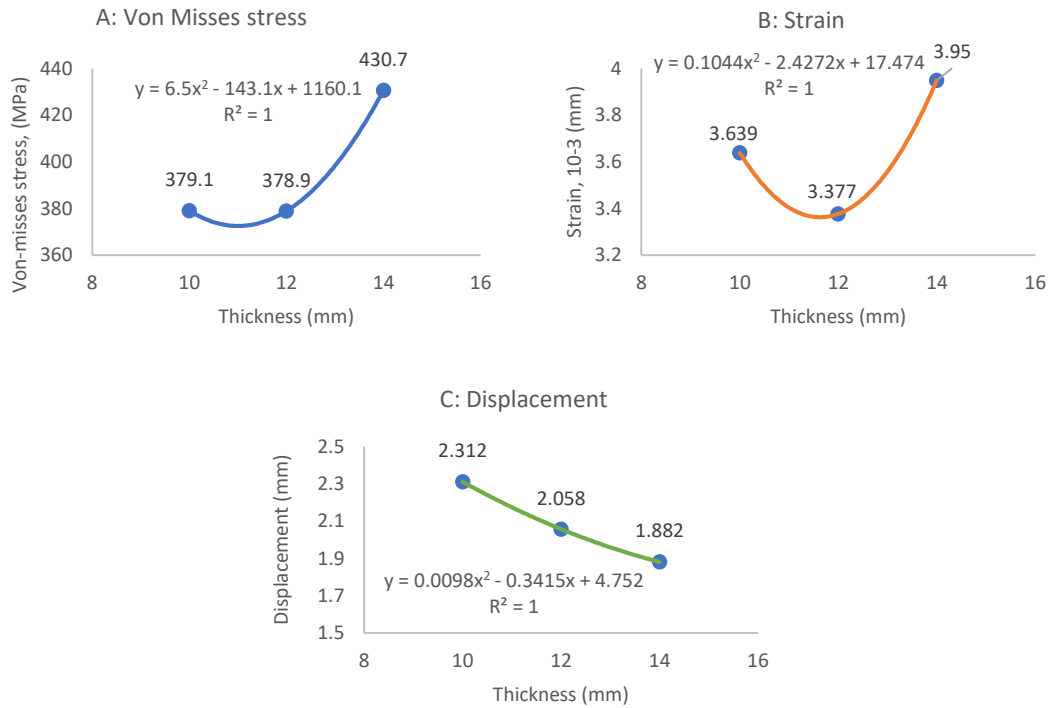
A: Von Misses stress

$y = 6.5x^2 - 143.1x + 1160.1$
$R^2 = 1$

430.7
379.1   378.9

B: Strain

$y = 0.1044x^2 - 2.4272x + 17.474$
$R^2 = 1$

3.95
3.639
3.377

C: Displacement

2.312
2.058
1.882

$y = 0.0098x^2 - 0.3415x + 4.752$
$R^2 = 1$

Figure 8: (a) maximum von Mises stress, (b) displacement, and (c) strain for thickness analysis.

3.3 Analysis of factor C: Width

In this analysis, only the width varies (28 mm, 30 mm, 32 mm), and the other factor is fixed on the level 2 value. All simulations are performed with an external load of 1000 N force. The result of von Mises stress, displacement, and strain are shown in Figures 9 (a), (b), and (c), respectively. Based on the graph shown in Figure 9 (a), the maximum von Misses stress on level 3 is the lowest compared to level 1. The highest stress for a 28mm width is 400.1 MPa meanwhile, for a 32 mm width is 364.1 MPa. The percentage of difference for both levels is approximately 4.72%. Based on the graph illustrated in Figure 9 (b), the strain on 32 mm width is the highest with 3.886×10^{-3} mm compared to 28 mm width (3.721×10^{-3} mm). The percentage difference for both structure levels in the y-direction is approximately 2.16%. This result clearly shows that a larger area will increase the strain amount of deformation experienced by the body in the direction of force applied. Based on the graph in Figure 9(c), the displacement of 32 mm width is the lowest (1.733 mm) compared to 28 mm width (2.436 mm). The percentage difference for both structure levels in the y-direction is approximately 16.86%. This result shows that a larger area will decrease the displacement of an object when the force is applied.
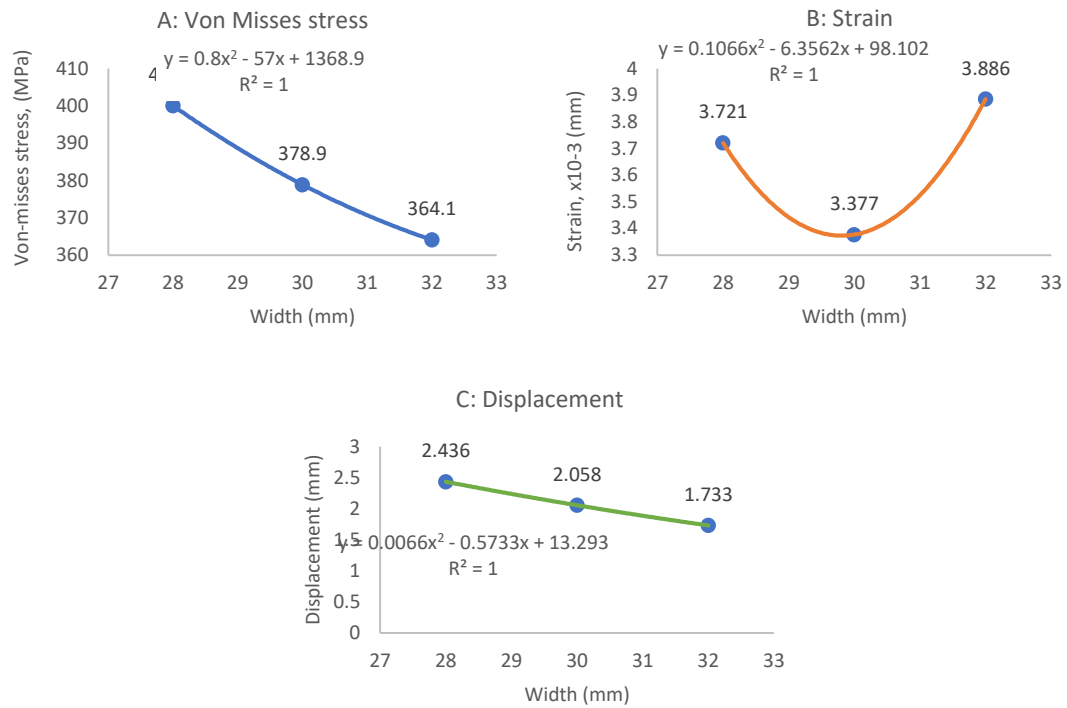
Figure 9: (a) maximum von Mises stress, (b) displacement, and (c) strain for width analysis.

3.4 Analysis of factor D: Numbers of the crank spider

In this analysis, 3, 4, and 5 crank spiders are used, and the other factor is fixed on the level 2 value. All simulations were performed with an external load of 1000 N force. The result of von Mises stress, displacement, and strain are shown in Figures 10 (a), (b), and (c), respectively. From the bar chart in Figure 10 (a), three spider cranks have the highest stress with 1125 MPa, and five spider cranks have the lowest stress with 469 MPa. In the y-direction, the percentage difference between both levels is roughly 41.16%. In Figure 10 (b), the strain on five crank spiders is the lowest (4.73×10^{-3} mm), and the highest is 9.152×10^{-3} mm for three crank spiders. The percentage difference between the two structural levels is 31.86%. In Figure 10 (c), the displacement for three crank spiders is the highest, with 4.431 mm, while 2.705 mm displacement for five crank spiders. The percentage variation in the y-direction for both structural levels is 24.21%. These findings indicate that increasing the area will reduce an object's displacement when applied force.
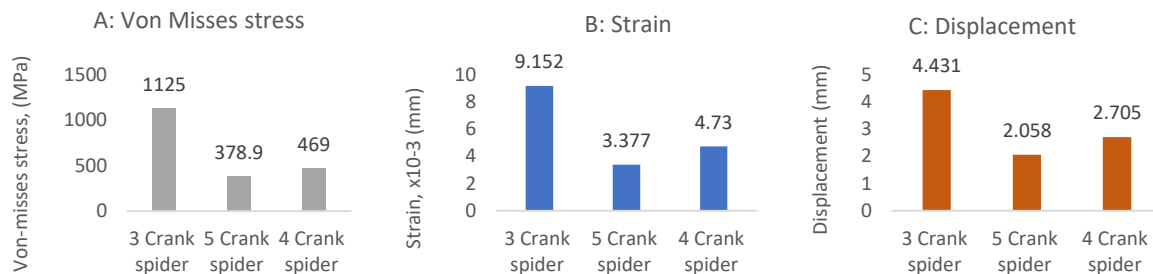

Figure 10: Comparison of the crank spider for (a) maximum von Mises Stress, (b) strain, and (c) displacement.
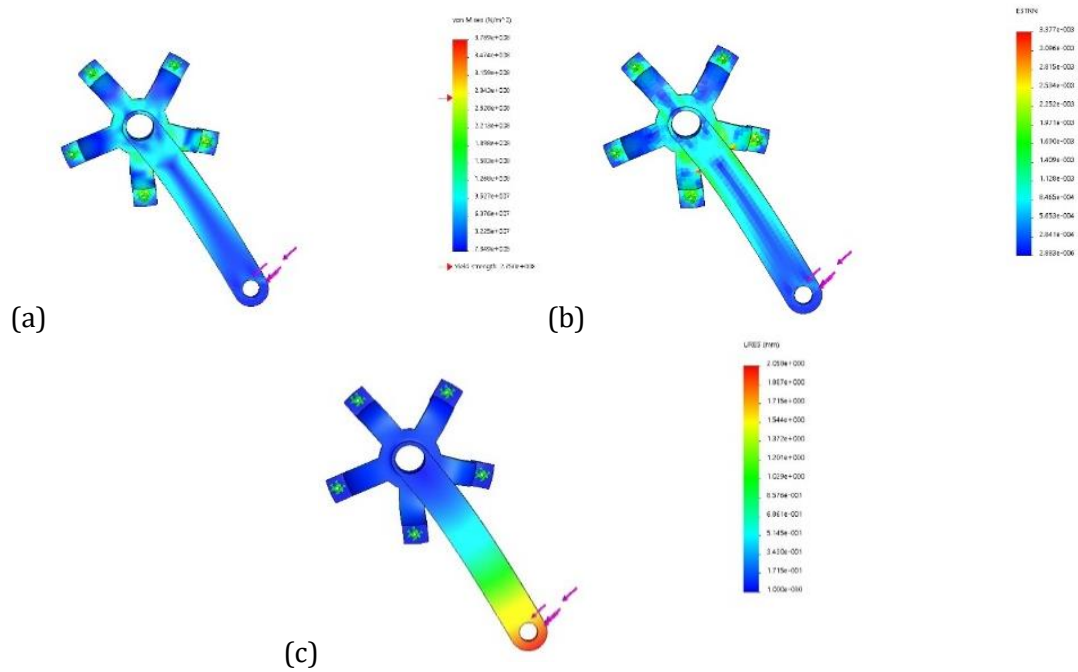
Figure 10: Simulation result for (a) maximum von Mises stress, (b) displacement, (c) strain with five crank spiders.

3.5 Analysis of factor E: Rib design

This section analyzes three rib designs: standard, slot, and pocket. All simulations were performed with an external load of 1000 N force. The result of von Mises stress, displacement, and strain are shown in Figures 11 (a), (b), and (c), respectively. Based on the graph shown in Figure 11 (a), the highest stress is for slot design with 634 MPa, while the lowest is for standard design with 399.7 MPa. The percentage difference is approximately 22.66%. For the strain result, as shown in Figure 11 (b), the lowest strain is 3.522×10^{-3} mm for standard design the highest is for slot design with 7.232×10^{-3} mm. The percentage difference is 34.5%. In Figure 11 (c), the displacement on the slot rib design is the highest at 6.477 mm compared to the standard design with 2. The percentage variation in y-direction for both structural levels is 44.86%. These results show that even though the slot design comes with the lightest weight, it has the highest stress, strain, and displacement when the force is applied. These results conclude that the standard design is slightly better than the pocket rib design. However, the pocket design is lighter than the standard design.
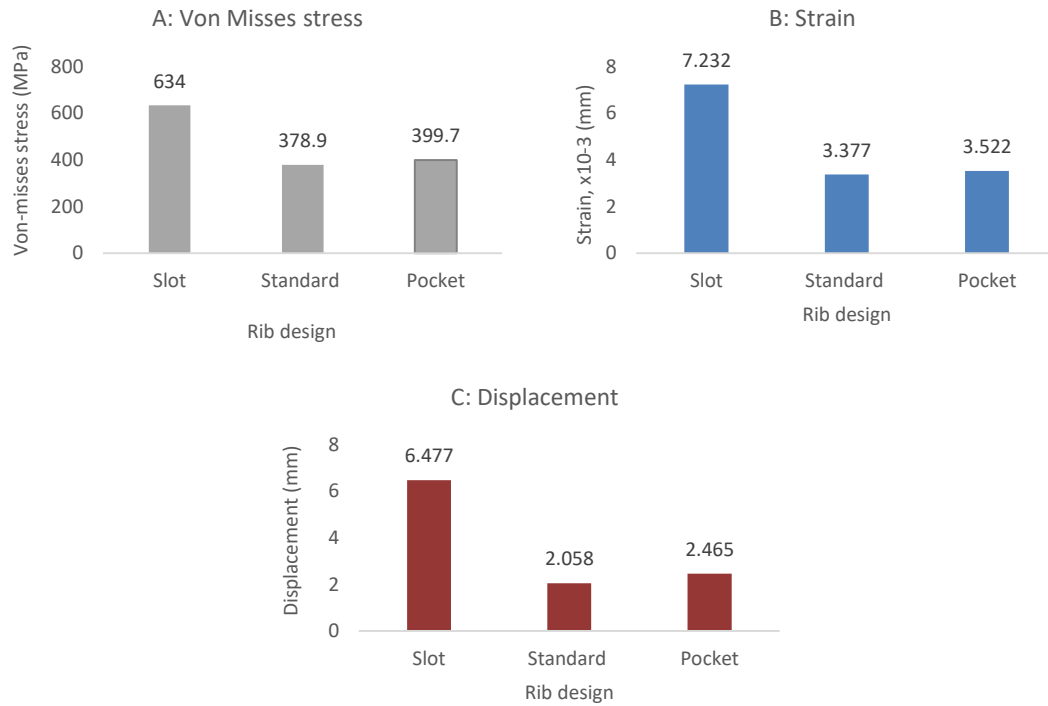
Figure 11: (a) Bar chart for maximum Von Mises Stress, (b) displacement, and (c) strain for rib design analysis.
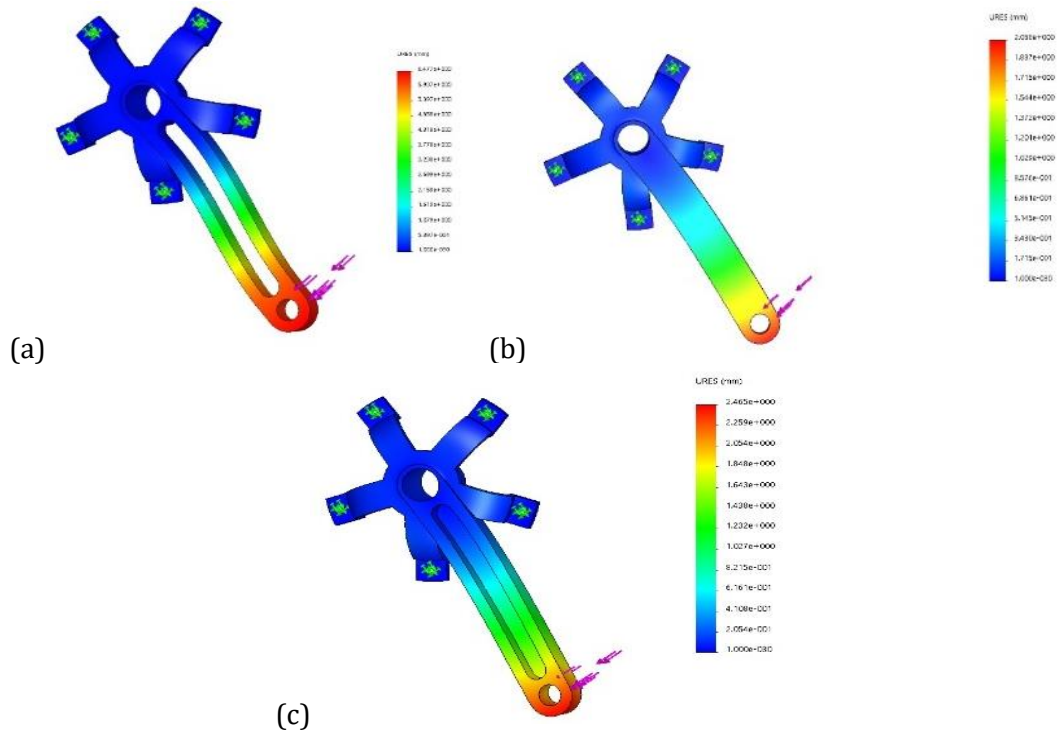

Figure 12: Simulation result of displacement for (a) slot design, (b) standard design, and (c) pocket design.

4. CONCLUSION

In this study, the effect of the design parameters on mechanical performance has been analyzed using finite element analysis. The selected parameters in this study are crank arm length, width, thickness, number of cranks spider, and rib design. Von Misses stress, strain, and displacement were the selected dependent variables for this study. The external load of 1000 N force was applied in the y-direction. Generally, the analysis results showed that 160 mm length, 30 mm width, and 10 mm thickness, including five crank spiders and pocket design arm, have the lowest stress, strain, and displacement. From the length analysis results, it can be concluded that increasing the length will increase the stress, strain, and displacement value. Crank arm thickness analysis results show that increasing the arm thickness will increase the stress and strain value. However, the displacement value decreased when the thickness increased. The width and number of spider analyses show that a larger cross-sectional area across the structure will decrease the displacement of an object when the force is applied. For the crank arm rib design, it concludes that the standard design is slightly better than the pocket rib design. However, the pocket design is lighter than the standard design. In conclusion, bringing a new alternative to the crank's arm structure can help improve the rigidity to produce complex 3D shapes precisely.

REFERENCES

[1] Siedentop, D., Hastie, P., & Van der Mars, H. Complete guide to sport education. Human Kinetics, (2019).

[2] Madivalar, C. N., & Shay, T. Fatigue Failure Analysis Of Bike Crank Arm Usi ng Solidworks Simulation. Journal of Mechanical Engineering Research & Developments, vol 41, issue 3 (2018)pp.9-13.

[3] Luqman, M., Rosli, M. U., Khor, C. Y., Zambree, S., & Jahidi, H. Manufacturing process selection of composite bicycle's crank arm using analytical hierarchy process (AHP). In IOP conference series: materials science and engineering vol 318, issue 1 (2018) p.012058.

[4] Gutiérrez-Moizant, R., Ramirez-Berasategui, M., Calvo, J. A., & Alvarez-Caldas, C. Validation and improvement of a bicycle crank arm based in numerical simulation and uncertainty quantification. Sensors, vol 20, issue 7 (2020) p.1814.

[5] Ismail, A. Y., Na, G., & Koo, B. Topology and response surface optimization of a bicycle crank arm with multiple load cases. Applied Sciences, vol 10, issue 6 (2020)p.2201.

[6] McEwen, I., Cooper, D. E., Warnett, J., Kourra, N., Williams, M. A., & Gibbons, G. J. Design & manufacture of a high-performance bicycle crank by additive manufacturing. Applied Sciences, vol 8, issue 8 (2018)p.1360.

[7] Htun, H. M., & Nyi, C. Z. N. Structural Analysis of Crank Arm for Quadracycle. International Journal of Science, Engineering and Technology Research (IJSETR), vol 8, issue 1 (2019) pp.1–5.

[8] Charan, D., & Garg, S. K. Design and Simulation of Bike Frame Using SolidWorks and ANSYS, vol 12, issue 7 (2019) pp.1074–1079.

[9] Ishak, M. I., Shafi, A. A., Rosli, M. U., Khor, C. Y., Zakaria, M. S., Rahim, W. M. F. W. A., & Jamalludin, M. R. Biomechanical evaluation of different abutment-implant connections–a nonlinear finite element analysis. In AIP Conference Proceedings, vol 1885, issue 1 (2017) p. 020064.

[10] Nawi, M. A. M., Amin, M. R., Kasim, M. S., Izamshah, R., Ishak, M. I., Khor, C. Y., ... & Syafiq, A. M. The influence of spiral blade distributor on pressure drop in a swirling fluidized bed. In IOP Conference Series: Materials Science and Engineering, vol 551, issue 1 (2019) p.012106.

[11] Khor, C. Y., Ishak, M. I., Rosli, M. U., Jamalludin, M. R., Zakaria, M. S., Yamin, A. F. M., ... & Abdullah, M. Z. Influence of material properties on the fluid-structure interaction aspects during molded underfill process. In MATEC web of conferences, vol 97, (2017) p. 01059.

[12] Burt, P. Bike Fit 2nd Edition: Optimise Your Bike Position for High Performance and Injury Avoidance. Bloomsbury Publishing, (2022).